AD-A133 736 WAVE ATTENUATION IN DAMPED PERIODIC STRUCTURES(U) 1/1
MINNESOTA UNIV MINNEAPOLIS DEPT OF AEROSPACE
ENGINEERING AND MECHANICS R PLUNKETT ET AL. 12 JUL 83
UNCLASSIFIED N00014-82-K-0591 F/G 20/1 NL

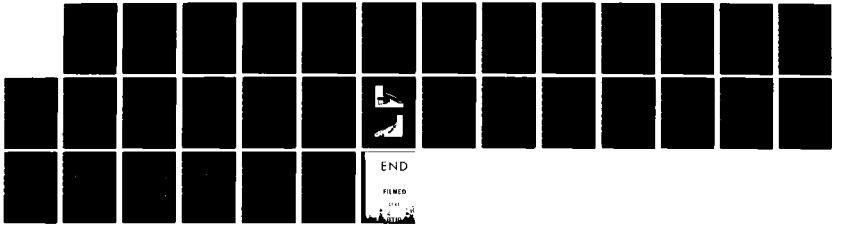

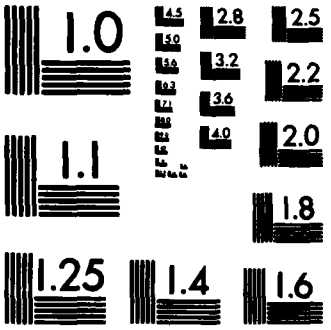

MICROCOPY RESOLUTION TEST CHART
NATIONAL BUREAU OF STANDARDS-1963-A

(2)

Wave Attenuation in Damped Periodic Structures

Robert Plunkett
Ajit K. Roy

Aerospace Engineering and Mechanics Department
University of Minnesota
Minneapolis, MN 55455

12 July 1983

Interim Technical Report
N00014-82-K-0591

Dr. N. L. Basdekas
Code 432 ONR
Technical Monitor

1. Introduction

It has been known for some time that periodic structures will act as filters for bending waves*. The equations for an infinite ribbed bar have been published with some limited confirming evidence**. The objective of this study is to get extensive quantitative results, both analytical and experimental, for a finite number of tuned ribs and to extend the work to plates and possibly shells. In the process, we intend also to investigate the differences between symmetric (two-sided) and asymmetric (one-sided) cantilever ribs. This first technical report gives analytical and experimental results for the uniform bar (unribbed) and for the same bar with fifteen pairs of tuned cantilevers which approximates the infinite ribbed bar. Section 2 gives the necessary equations, Section 3 describes the experimental methods, Section 4 discusses the results (good agreement!) and Section 5 describes future work.

The work has been facilitated by a number of discussions with the Technical Monitor, Dr. N. L. Basdekas.

---

* G. SenGupta "Vibration of Periodic Structures" Shock and Vibration Digest, 12, 3, 1980, pp. 17-31.

** Gruzin, V. V., V. P. Kandidov and V. I. Shmalgavzen "Filtering of Elastic Waves in a Bar with Ribs". Izv. AN SSSR. Mek. Tverd. Tela. 12, 4, pp. 180-184, 1977, Trans. Allerton Press, 1977.

2. Analysis

2.1 Uniform Beam.

The Bernoulli-Euler differential equation for bending wave propagation in a uniform beam is*:

$$D\frac{\partial^4 y}{\partial x^4} + \rho A \frac{\partial^2 y}{\partial t^2} = 0 \qquad (2.1.1)$$

If we assume a sinusoidal wave traveling to the right:

$$y = a \exp i(kx-\omega t) \qquad (2.1.2)$$

and substitute into equation 2.1.1, we get:

$$k^4 D - \rho A \omega^2 = 0 \qquad (2.1.3)$$

This shows that the wave is dispersive with the phase velocity given by

$$C = \frac{\omega}{k} = (\omega^2 EI/\rho A)^{1/4}$$

$$= (\omega t C_r/\sqrt{12})^{1/2} \qquad (2.1.4)^{**}$$

where

$D = EI$ is the bending stiffness

ω = frequency in rad/sec

t = beam thickness for a rectangular cross section

$C_r = \sqrt{E/\rho}$ is the rod phase velocity

Thus, if we have a bending wave traveling to the right and the bending strain at x as a function of time is:

$$\varepsilon(x, t) = f(x, t) \qquad (2.1.5)$$

---

* W. Goldsmith "Impact" Arnold, London 1960, eq. 3.118

** The anticlastic curvature restraint is not effective for a thin rectangular cross section at small strain levels and so the $1-D^2$ term is omitted.

we can find the time function at $x + x_o$ by taking the Fourier transform of f, shifting the phase by $\omega T = \omega x_0/C$ and taking the inverse transform. Thus:

$$F(x, \omega) = \frac{1}{2\pi} \int_{\infty}^{\infty} f(x, t) \exp(-i\omega t)dt \qquad (2.1.6)$$

$$F(x + x_o, \omega) = F(x, \omega)\exp(i\theta) \qquad (2.1.7)$$

$$\theta = \omega x_o/C = x_o(\omega\sqrt{12}/tC_r) = \theta_o\sqrt{f/f_o} \qquad (2.1.8)$$

where θ_o is the phase shift at the reference frequency f_o

$$\text{and } f(x + x_o, t) = \int_{-\infty}^{\infty} F(x + x_o, \omega) \exp(i\omega t)dt \qquad (2.1.9)$$

The time history of the bending wave computed from equation 2.1.9 is compared with the measured one in section 4, Results.

2.2 Periodic Beam

A periodic structure was constructed by fastening double cantilevers to the uniform beam at equal intervals, fig. 2.2.1.

We can analyse a traveling wave in a infinite periodic structure by considering the boundary conditions at each end of one section of the beam, fig. 2.2.2. If we have a wave of frequency ω traveling in an undistorted fashion, it must attenuate by the same fraction in each section. If we assemble the four components of force and displacement into one vector

$$y_i = \begin{Bmatrix} v_i \\ \theta_i \\ M_i \\ -F_i \end{Bmatrix} = \begin{Bmatrix} v_i \\ v_i' \\ EIv'' \\ EIV''' \end{Bmatrix} \qquad (2.2.1)$$

we may write

$$y_{i+1} = \lambda y_i \tag{2.2.2}$$

where λ is the ratio between each two successive periodic repeats. If we now find the components at one end in terms of those at the other

$$z_{i+1} = Hz_i = \lambda z_i \tag{2.2.3}$$

then we have an eigenvalue problem where H is a function of frequency. We can find H from the solution for the uniform beam (fig. 2.2.3) with the sign conventions shown in figures 2.2.2 and 2.2.3; our equations of equilibrium at point i are

$$\begin{aligned} F_i &= F_{1i} - P_{2i} + P_{3i} \\ M_i &= M_{1i} - M_{2i} - M_{3i} \\ P_i &= P_{1i} + F_{2i} - F_{3i} \end{aligned} \tag{2.2.4}$$

Compatibility for deflection and slope is automatically satisfied by the conventions shown. In addition to the bending wave equation (eq. 2.1.1), there is an extensional wave equation

$$EA \frac{\partial u}{\partial x} + \rho A \frac{\partial^2 u}{\partial t^2} = 0 \tag{2.2.5}$$

For a sinusoidal wave of frequency ω, the general solution of equation 2.1.1 for the beam piece is

$$v = A \cosh \beta x + B \sinh \beta x + C \cos \beta x + D \sin \beta x \tag{2.2.6}$$

where $$\beta^4 = 12 \rho \omega^2 / Et^2 \tag{2.2.7}$$

so that $v' = A\beta \sinh \beta x + B\beta \cosh \beta x - C\beta \sin \beta x + D\beta \cos \beta x$

$$M/EI = v'' = A\beta^2 \cosh \beta x + B\beta^2 \sinh \beta x - C\beta^2 \cos \beta x - D\beta^2 \sin \beta x$$

$$F/EI = v''' = A\beta^3 \sinh \beta x + B\beta^3 \cosh \beta x + C\beta^3 \sin \beta x - D\beta^3 \cos \beta x$$

Substituting in x = L, solving for A, B, C and D then substituting in x=0 we find that

$$z_i = G z_{i+1} \tag{2.2.8}$$

where G is given by equation A.6 in the Appendix and we have changed the definition of z to

$$z_i = \begin{Bmatrix} v_i \\ v_i'/\beta \\ M_i/EI\beta^2 \\ -F_i/EI\beta^3 \end{Bmatrix} \tag{2.2.9}$$

If we now make the change to local coordinates for the short cantilevers, and put in the boundary conditions

$$M = 0 \text{ and } F = 0 \text{ at } x = h$$

we get

$$\begin{Bmatrix} M_{2i}/EI\beta^2 \\ F_{2i}/EI\beta^3 \end{Bmatrix} = A \begin{Bmatrix} v_{i2} \\ v'_{i2}/\beta \end{Bmatrix} \tag{2.2.10}$$

where A is equation A.1 in the appendix. The corresponding solution for equation 2.2.5 is

$$u = E \cos \gamma x + F \sin \gamma x \tag{2.2.11}$$

where $\gamma = \omega/c_r$.

Using the fact that $P = AE\,u'$, solving for E and F in terms of P_{i+1} and U_{i+1}, we find that

$$\begin{Bmatrix} u_i \\ P_i \end{Bmatrix} = B \begin{Bmatrix} u_{i+1} \\ P_{i+1} \end{Bmatrix} \tag{2.2.12}$$

If we now change to local coordinates and put in the boundary condition that P=0 at $x_2 = h$, we find that

$$P_{2i} = \tan \alpha_3 \; u_{2i} \tag{2.2.13}$$

where $\alpha_3 = h/c_r$. Substituting from equations 2.2.8, 2.2.9, 2.2.10, 2.2.12 and 2.2.13 into 2.2.4, we finally get that

$$H = \left| \begin{array}{c|c} C + D & O \\ \hline O & G + F \end{array} \right| \tag{2.2.14}$$

where B, C, D, G and F are given in the Appendix and now

$$Z_i = \begin{Bmatrix} u_i \\ P_i/\rho EA \\ v_i \\ \theta_i/\beta \\ M_i/EI\beta^2 \\ -F_i/EI\,\beta^3 \end{Bmatrix} \tag{2.2.15}$$

Because of symmetry, there is no coupling between the first two and the last four terms so that we may solve a 4x4 eigenvalue problem. If the cantilevers and the beam are the same thickness and made from the same material, the only parameter remaining

is the ratio h/L. If h/L = 0.470, and it does for our experiment, $\alpha_4 = 0.470\alpha_2$ and we may solve for λ as a function of α_2^2, the dimensionless frequency. At each frequency there are four roots λ which occur in pairs corresponding to right and left traveling waves. There are three possible types of root pairs:

1) conjugate complex, modulus 1;

2) two pairs of conjugate complex roots (4 roots total) in which the modulus of one is the reciprocal of that of the other;

3) two real reciprocal roots.

Type 1 governs an unattenuated pair of waves, one traveling right and one left. Type 2 governs two stationary waves, in each direction one wave is increasing and one is attenuating. Type 3 governs two stationary, exponential modes; one is damping and one growing for positive x and they reverse roles for negative x similar to the stationary oscillatory modes of type 2. Our solution is strictly valid only for an infinite set of cantilevers. If any of the roots are of type 1, at least some of the bending energy will propagate unattenuated. If all of the roots are of types 2 or 3, then all of the bending energy will be attenuated by multiple reflections. The eigenvalues and eigenvectors were found numerically as a function of ω on a CDL Cyber 176 using the IMSL routine EIGCC. If we express the complex λ's in polar form, the argument is the phase shift of the eigenvector. Figure 2.2.4 shows a plot of the phase shift as a function of frequency for L = 5.00 in, h = 2.47 in., $E = 3 \times 10^7$ psi and t = 0.25 inch for a steel bar. The passbands and stop bands are also indicated for comparison with the

measured values. As can be seen, type 3 stop bands are necessarily 0° ($\cos\theta = 1$) or 180° ($\cos\theta = -1$) phase shift.

3. Experimental Technique

3.1 Instrumentation

The bending waves were detected by a pair of strain gages on opposite sides of the beam connected to Vishay 1011 signal conditioners. The dynamic output was then connected to the input terminals of a Hewlett Packard 3582A Spectrum analyser and, in parallel to the input of a Nicollet 3091 digital oscilloscope (Fig. 3.1.1). A HIPlot x-y recorder was used to make hard copies of the stored signals. The oscilloscope has a pretrigger feature which can be set to show the signal which occured up to one full time sweep of the screen before the trigger; the Spectrum Analyser does not have a pretrigger feature. The bending wave in the beam was excited by a simple pendulum with a spherical bob (fig. 2.2.1). A photodiode was illuminated by a focussed light beam (not shown in fig. 2.2.1) which was interrupted by the pendulum extension. The step signal from the photodiode was used to externally trigger the analyser; the pre-impact time was adjusted by moving the light beam away from the impact point.

3.2 Beam

A uniform steel beam, 0.250 inch thick by 2.00 inch wide and 36 feet long was hung in a horizontal position by 0.030 inch piano wires fastened at 4 foot intervals to the thin edge by welding to 3/4 inch, 6-32 screws in drilled and tapped holes; the screws were locked by locknut. The wires were fastened to an overhead pipe 4 feet above and adjusted by turnbuckles

to equal tension by tuning to the same note. The impact point was 16 feet from one end. The traveling waves were measured at point A, 10 inches from the impact point and point B, 82 inches from the impact point, both on the 20 foot end.

After the uniform beam measurements, 15 pairs of cantilevers each 2.35 inch long were fastened to the beam at 5 inch intervals starting one inch from position A. Each pair was tested on a short beam 2 inches long on a vibration shaker. After the bases of the cantilevers and the milled surfaces of the support had been carefully polished with 400 grit emery paper, the natural frequencies were measured to be between 1332 and 1386 Hz, both cantilevers of a pair had the same phase angle at resonance within 3° and the estimated η was less than 0.003. The resonant frequency of a 2.35 inch cantilever calculated by using the phase velocity measured later is 1394 Hz; if we assume the length (arbitrarily) to be 2.40 inch to account for the elasticity of the base, we get 1340 Hz.

3.3 Measurements Made

3.3.1 Uniform Beam

As stated, the uniform beam was 36 feet long with strain gage bridges at 10 inches and 82 inches from the input point. The impact point was 16 feet from the other end. No attempt was made to measure the bending pulse immediately under the impact point. Standard impacts were repeated at the impact point for 10 time spectrum averages of channels A (10 inch) and B (82 inch) with gain settings at 30 mv max, frequency

range 10 kHz (12.5 ms time signal) and AC coupling. The light beam was moved to trigger the spectrum analyser 4.5 m sec before impact. This time was chosen just long enough to make the coherence almost 1.0 for the full frequency range while making the low frequency cutoff for point B as low as possible. We assume that difficulties at shorter time delays are caused by reflections from the free ends. Records were made of the A and B spectra (Fig. 3.2.1) and magnitude and phase of the transfer function (B/A spectra), figures 3.2.2 and 3. Figure 3.2.3 shows a plot of the unwrapped argument (phase) with an arbitrary zero. The transfer function is 1 within $\pm$ 0.5 dB from 2.5 kHz to 10 kHz except for small blips at about 4 and 8 KHz. The travel time after impact was 12.5 - 4.6 or 7.9 msec. This is the phase velocity travel time for 82 inches for a 1 kHz wave so the rolloff shown in figure 3.2.1 is appropriate.

A hard copy of a 13.4 msec time trace with about a 0.5 msec time delay was recorded from the digital oscilloscope, fig. 3.2.4.

3.3.2 Beam with cantilevers

The time delay was left at 4.6 msec to make sure that the signal was the same as in the previous section while the spectrum from Channel A was observed, it was not recorded since there is no convenient way to separate the incident wave from the reflected wave. The spectrum modulus at point B was recorded for the same amplitude settings as in the previous section. The 10 kHz (12.5 msec) spectrum and coherence are shown in figures

3.3.1 and 3.3.2 with a time delay of 4.4 msec. Those for 5 kHz (25 msec) and 2.5 kHz (50 msec) are shown in figures 3.3.3, 3.3.4 and 3.3.5 with longer time delays appropriate to the longer time signals. The predicted pass bands are shown in all figures; the longer time signals were taken to show the pass band from 0 to 856 Hz.

4. Results

4.1 Uniform Beam

The phase velocity of bending waves in a uniform beam is proportional to the square root of the frequency (equation 2.1.4) so that the beam is a dispersive medium for bending pulses. As a result, the time history of a given pulse depends on how far the pulse has traveled. In section II, we found that

$$C = (\omega t c_r/\sqrt{12})^{1/2} \qquad (2.1.4)\ \text{bis}$$

The phase shift for two spectra a distance L apart is

$$\theta = -\omega t = -\omega L/C \qquad (4.1.1)$$

From figure 3.2.3, $\theta = -88.25\sqrt{f}$ degrees for 72 inches. Substituting this value into equations 4.1.1 and 2.1.4, we find C_r = 190,400 inch/sec or E = 26.7×10^6 psi.

The phase velocity C is then 29,400 inch/sec at 10 kHz and the group velocity is twice that or 58,800 inch/sec. It should take 1.22 msec to travel 72 inches which agrees quite well with figure 3.2.4.

Goldsmith* shows that the force-time history of a sphere impacting on a beam is approximately a half sine pulse. A 16 point half sine pulse was FFTed over a 1024 point time interval, the phase of the spectrum shifted proportional to the square root of the frequency and the inverse FFT taken. Figure 4.1.1 shows the calculated time trace for a 56.6 radian shift at the highest frequency; figure 4.1.2 shows it for a 464 radian

---

* W. Goldsmith, "Impact" Arnold, London, 1960, fig 57, p. 119

shift (82/10 * 56.6 = 464). The 56.6 radian shift was chosen to make the ratio of the positive spike and the negative spike agree with that of figure 3.3.4. The qualitative agreement is gratifying but the analysis in detail is yet to be made. It is clear that the pulse shape cannot be exactly a half sine wave.

As was mentioned in Section 3.2, the transfer function is almost never less than -0.5 dB; the wave length of a 10 kHz bending wave is about 3 inches which gives 288 waves in a 72 inch distance which corresponds to a damping factor of less than 4×10^{-4} which is reasonable. Of course, the damping could not be measured to this accuracy for lower frequencies and longer wave lengths.

4.2 Periodic Beam

Fifteen sets of cantilevers give a reasonable approximation to an infinite periodic beam stop band (figures 3.3.1, 3.3.3, 3.3.5) with a maximum attenuation of about 25 dB. A close examination shows some attenuation at each end of the pass band and little attenuation in the stop band from 6263 to 6582. This will be investigated in future work.

5. Future Work

5.1 Finite Length

The analysis of Section 2 is now being extended to a finite number of cantilevers. This is being accompanied by experimental work. A first quick look shows appreciable attenuation at some frequencies with as few as three cantilevers but the spectra are not nearly as smooth as the ones shown here.

The next step will be to investigate the effects of assymmetric assemblies so that there is coupling between longitudinal and bending waves. In addition, the ratio of L to h will be changed by leaving out cantilevers.

5.2 Impedance Measurements

We also plan to make impedance measurements to investigate the possibility of steady state experiments which are simpler and more accurate than transient ones. If this can be perfected it will make measurements in ribbed plates and shells easier to interpret. We will need information on both input and transfer impedance to cope with those problems of reflection which have been avoided in the transient measurements.

Appendix

$$\beta^4 = \frac{\rho A \omega^2}{EI} \qquad \beta^2 = \frac{\omega\sqrt{12}}{C_r t} \qquad C_r^2 = \frac{E}{\rho}$$

$$\alpha_1 = \omega L / C_r \qquad \alpha_2 = \beta L \qquad \alpha_3 = \omega h / C_r \qquad \alpha_4 = \beta h$$

$$\Delta = 1 + \cosh\alpha_4 \cos\alpha_4$$

$$A = \frac{1}{\Delta}\begin{vmatrix} \sinh\alpha_4 \sin\alpha_4 & \cosh\alpha_4 \sin\alpha_4 - \sinh\alpha_4 \cos\alpha_4 \\ -\cosh\alpha_4 \sin\alpha_4 + \sinh\alpha_4 \cos\alpha_4 & -\sinh\alpha_4 \sin\alpha_4 \end{vmatrix} \qquad A.1$$

$$B = \begin{vmatrix} \cos\alpha_3 & \sin\alpha_3 \\ -\sin\alpha_3 & \cos\alpha_3 \end{vmatrix} \qquad A.2$$

$$C = \begin{vmatrix} \cos\alpha_1 & \sin\alpha_1 \\ -\sin\alpha_1 & \cos\alpha_1 \end{vmatrix} \qquad A.3$$

$$D = \frac{1}{\Delta}\begin{vmatrix} 0 & -\frac{2\omega}{\beta C_r}(\cosh\alpha_4 \sin\alpha_4 + \sinh\alpha_4 \cos\alpha_4)\cos\alpha_1 \\ -\frac{2\omega}{\beta C_r}(\cosh\alpha_4 \sin\alpha_4 + \sinh\alpha_4 \cos\alpha_4)\sin\alpha_1 & 0 \end{vmatrix} \qquad A.4$$

$$G = \begin{vmatrix} \cosh\alpha_2 + \cos\alpha_2 & \sinh\alpha_2 + \sin\alpha_2 & \cosh\alpha_2 - \cos\alpha_2 & \sinh\alpha_2 - \sin\alpha_2 \\ \sinh\alpha_2 - \sin\alpha_2 & \cosh\alpha_2 + \cos\alpha_2 & \sinh\alpha_2 + \sin\alpha_2 & \cosh\alpha_2 - \cos\alpha_2 \\ \cosh\alpha_2 - \cos\alpha_2 & \sinh\alpha_2 - \sin\alpha_2 & \cosh\alpha_2 + \cos\alpha_2 & \sinh\alpha_2 + \sin\alpha_2 \\ \sinh\alpha_2 + \sin\alpha_2 & \cosh\alpha_2 - \cos\alpha_2 & \sinh\alpha_2 + \sin\alpha_2 & \cosh\alpha_2 + \cos\alpha_2 \end{vmatrix} \qquad A.6$$

$$F = \begin{vmatrix} 0 & 0 & 0 & 0 \\ 0 & 0 & 0 & 0 \\ a(\sinh\alpha_2 - \sin\alpha_2) & a(\cosh\alpha_2 + \cos\alpha_2) & a(\sinh\alpha_2 + \sin\alpha_2) & a(\cosh\alpha_2 - \cos\alpha_2) \\ b(\cosh\alpha_2 + \cos\alpha_2) & b(\sinh\alpha_2 + \sin\alpha_2) & b(\cosh\alpha_2 - \cos\alpha_2) & b(\sinh\alpha_2 - \sin\alpha_2) \end{vmatrix} \quad A.5$$

$$a = \frac{\cosh\alpha_4 \sin\alpha_4 - \sinh\alpha_4 \cos\alpha_4}{1 + \cosh\alpha_4 \cos\alpha_4}$$

$$b = \frac{2\beta_n \tan\alpha_3}{\omega}$$

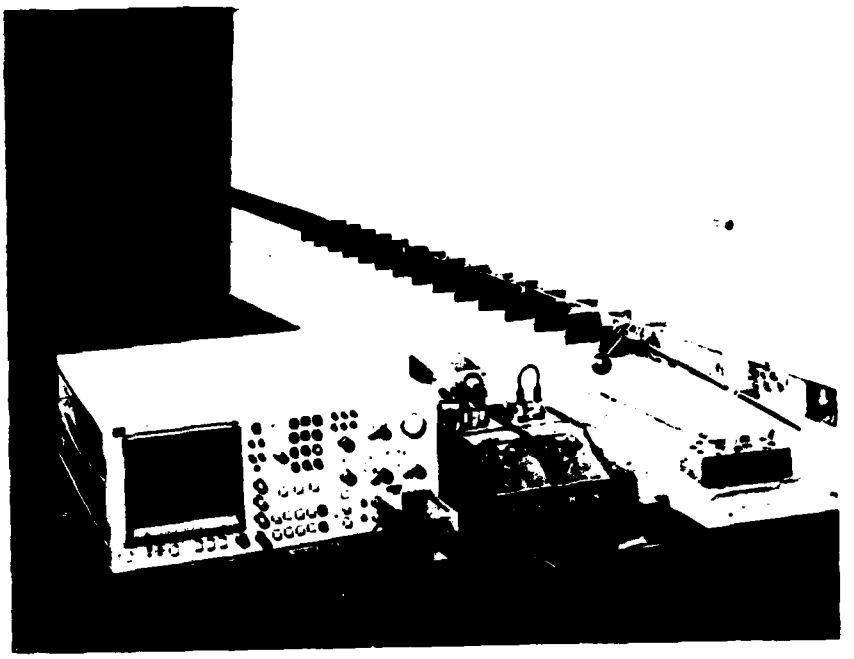

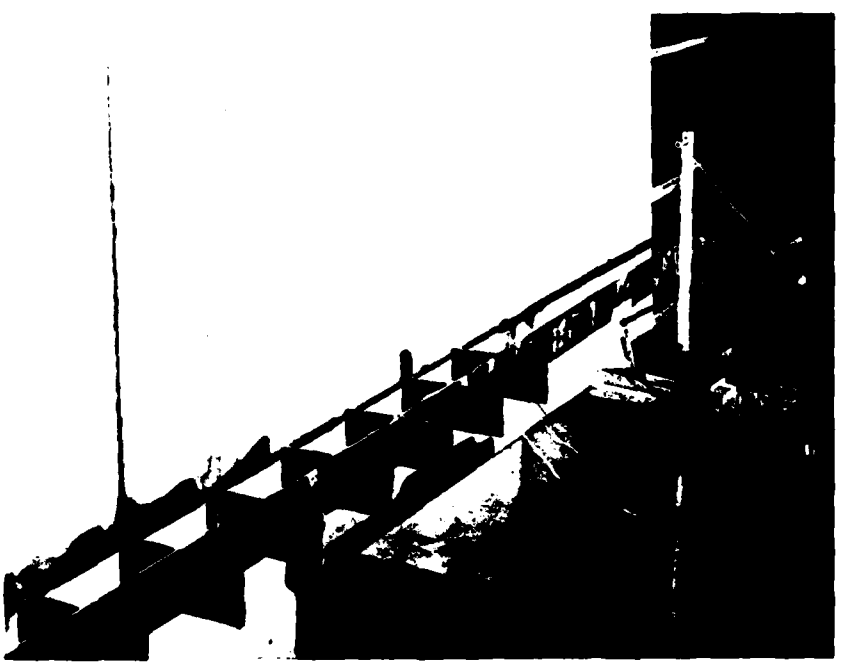

FIG 2.1.1

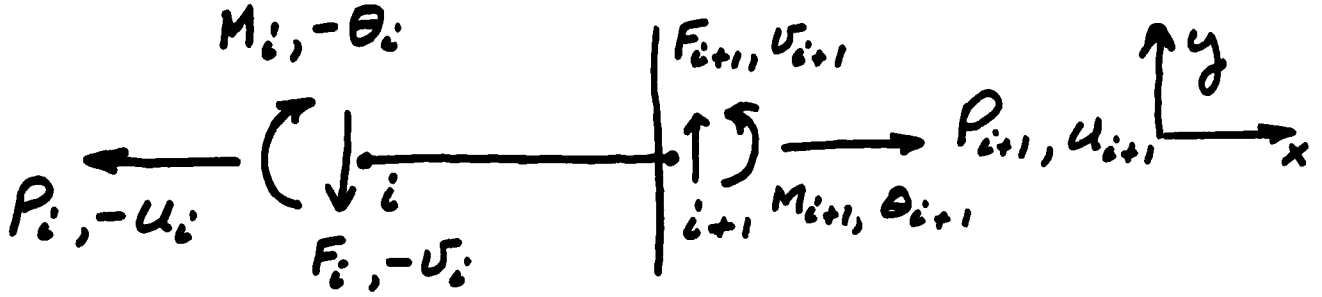

FIG 2.2.2

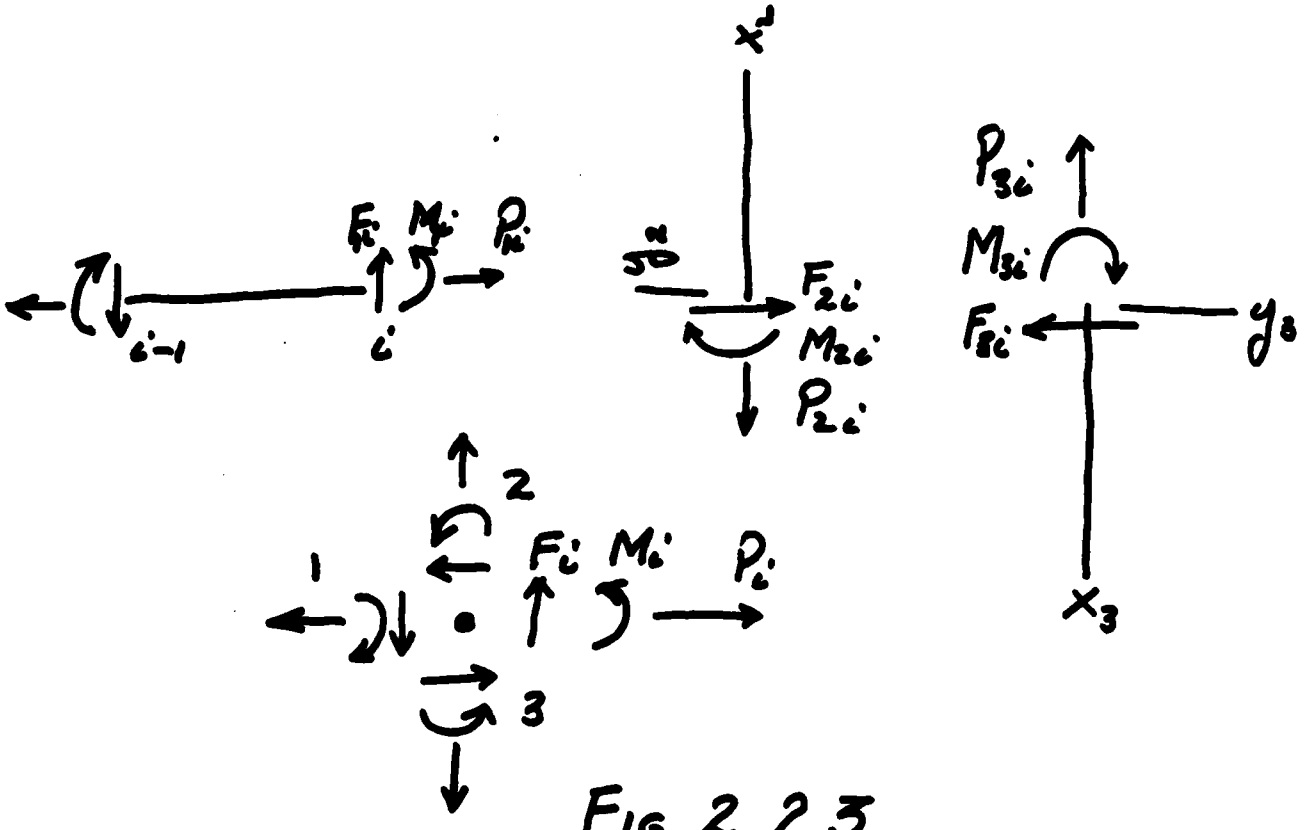

FIG 2.2.3

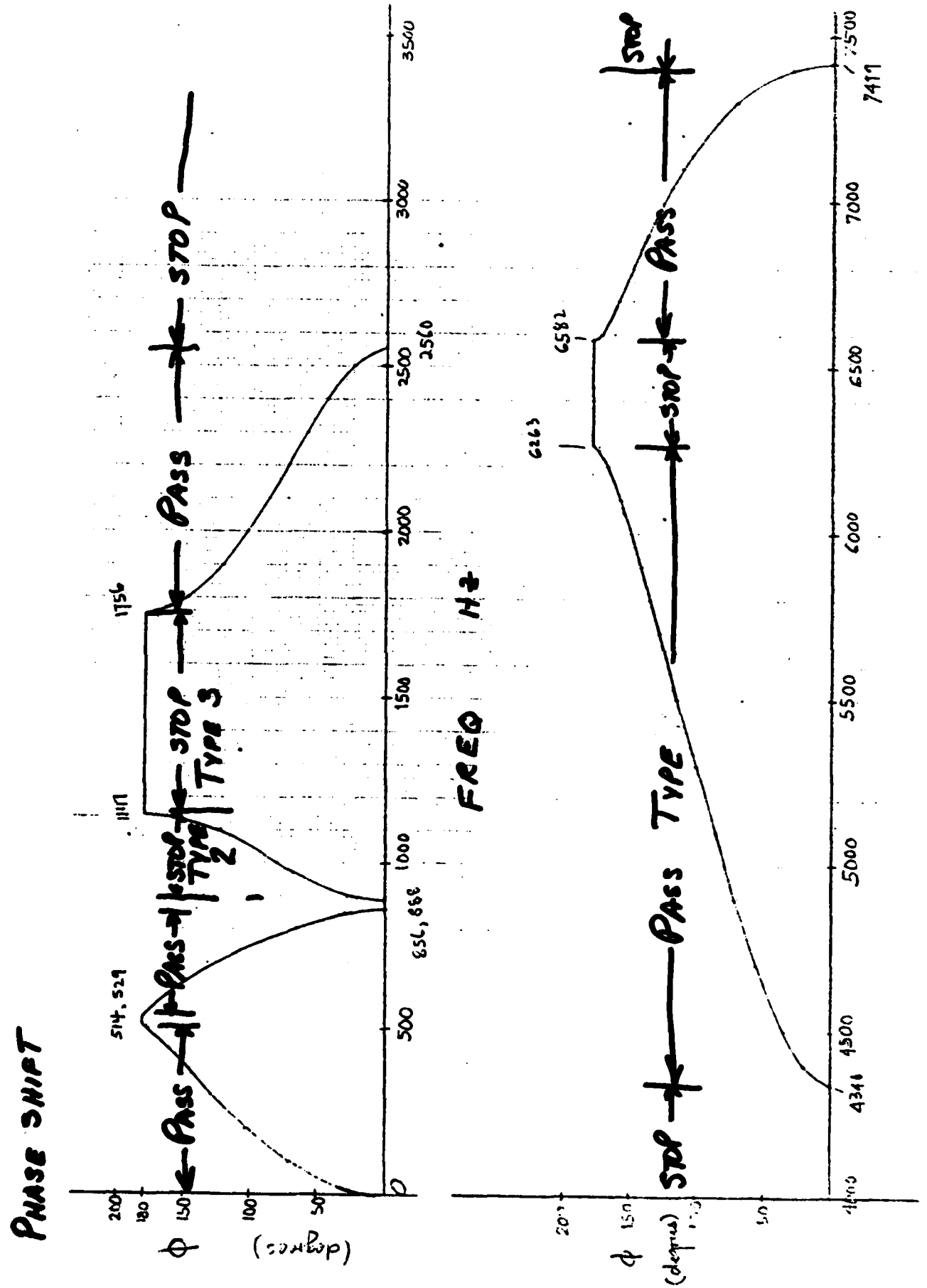
PHASE SHIFT
PASS
PASS
STOP
STOP
TYPE 2
TYPE 3
STOP
PASS
STOP
FREQ Hz
STOP
PASS
PASS TYPE
STOP
514, 529
1111
1756
651, 668
6263
6582
4341
7411
φ (degrees)
φ (degrees)

FIG 2.2.4

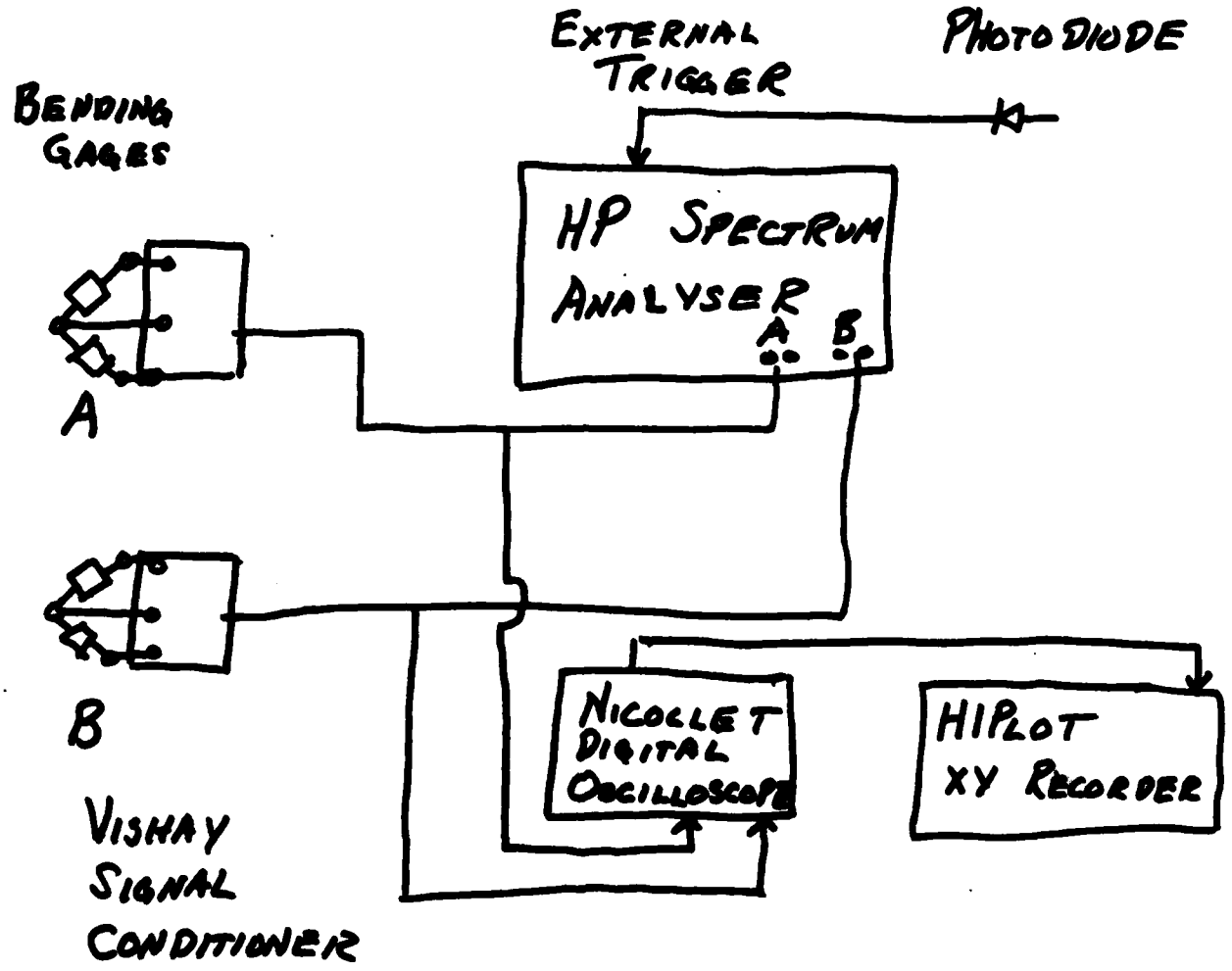
EXTERNAL TRIGGER
PHOTO DIODE
BENDING GAGES
HP SPECTRUM ANALYSER
A
B
A
B
NICOLLET DIGITAL OSCILLOSCOPE
HIPLOT XY RECORDER
VISHAY SIGNAL CONDITIONER

FIG 3.1.1

Figure 3.21 ms

7/11/83

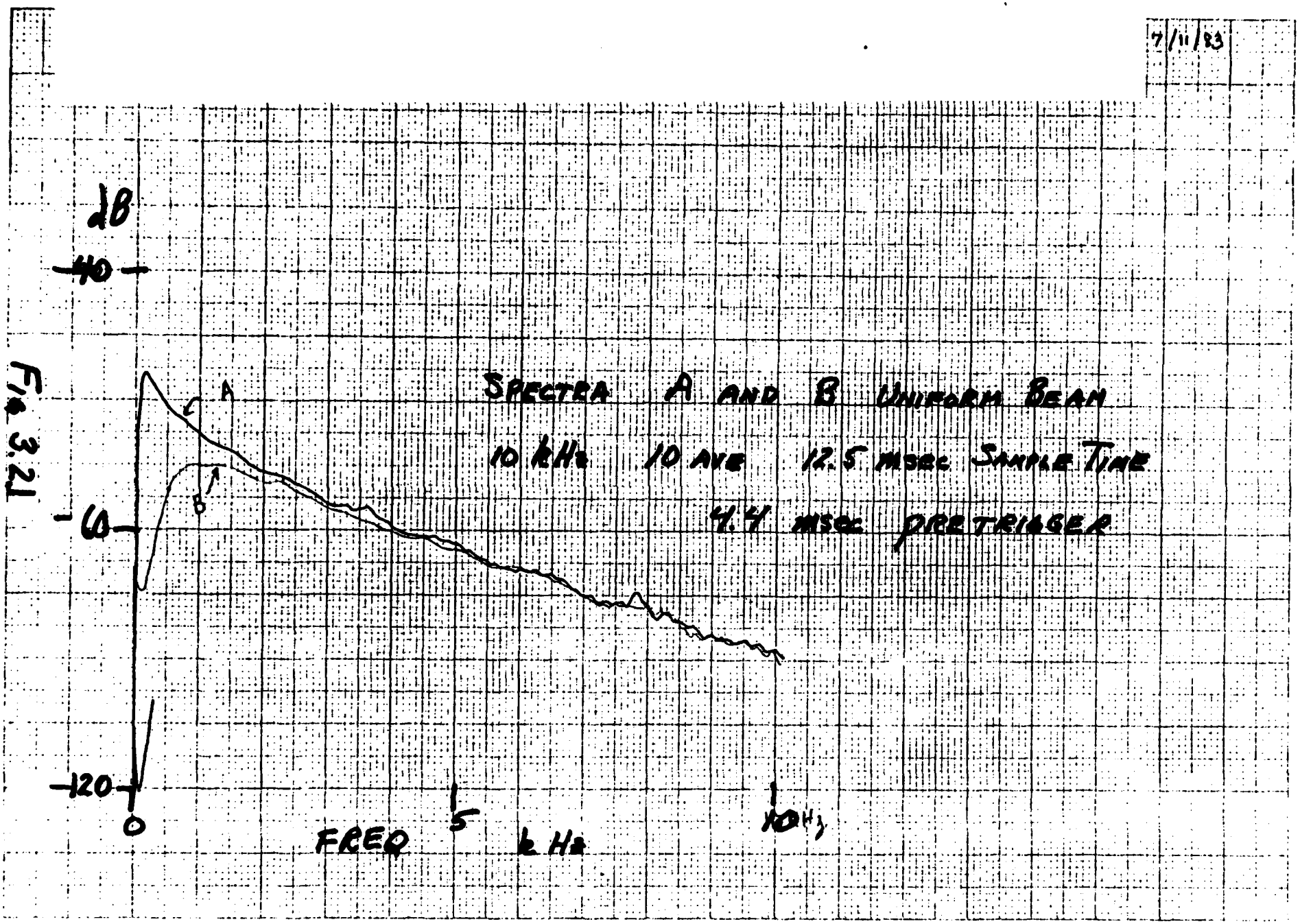

Fig. 3.21

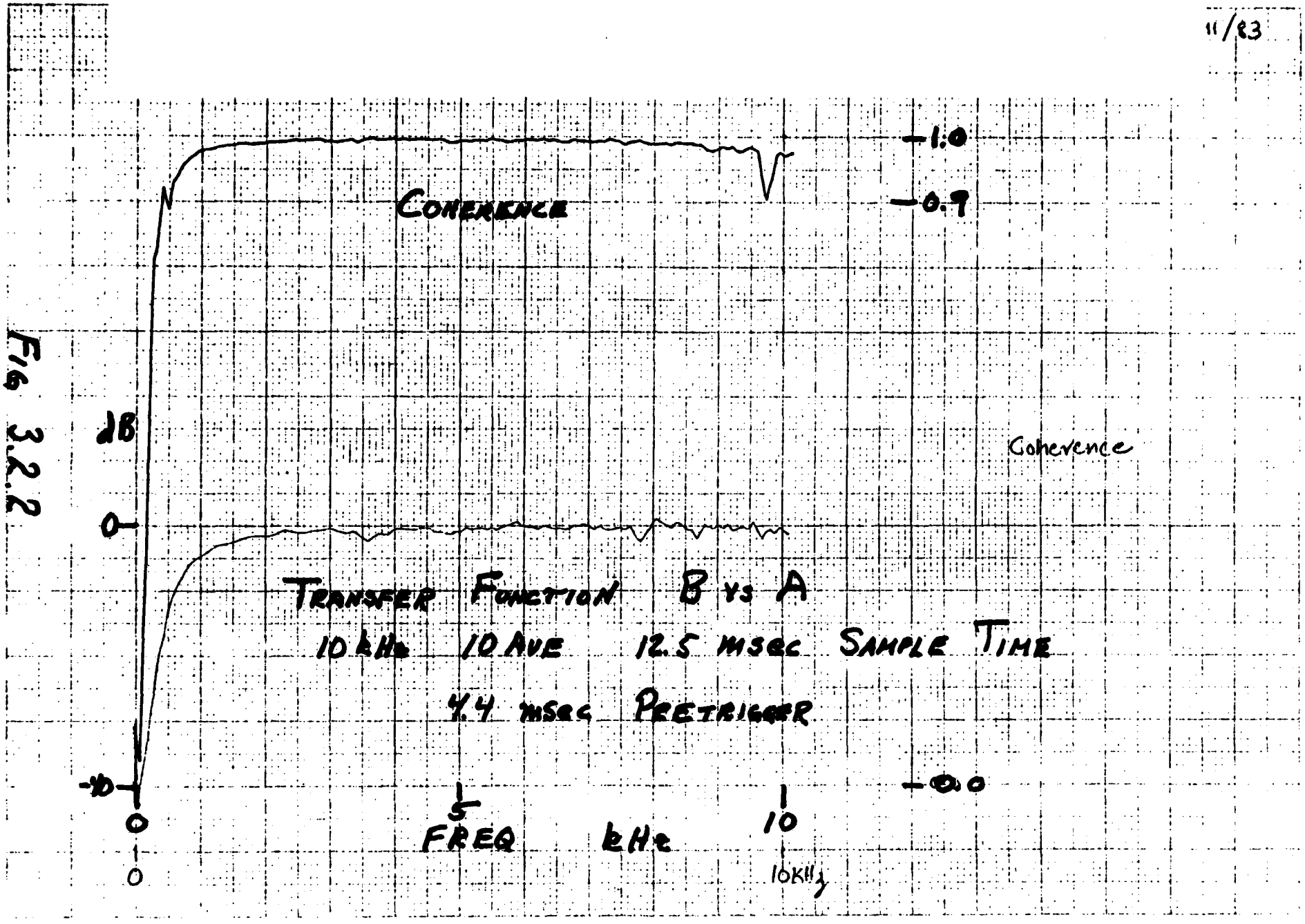
1.0
0.9
COHERENCE
dB
0
-10
0
0
Conevence
TRANSFER FUNCTION B vs A
10 kHz 10 AVE 12.5 MSEC SAMPLE TIME
4.4 MSEC PRETRIGGER
0.0
1/5
FREQ kHz
1/10
10KHz

FIG 3.2.2

Fig 3.2.3

Fig 3.2.4

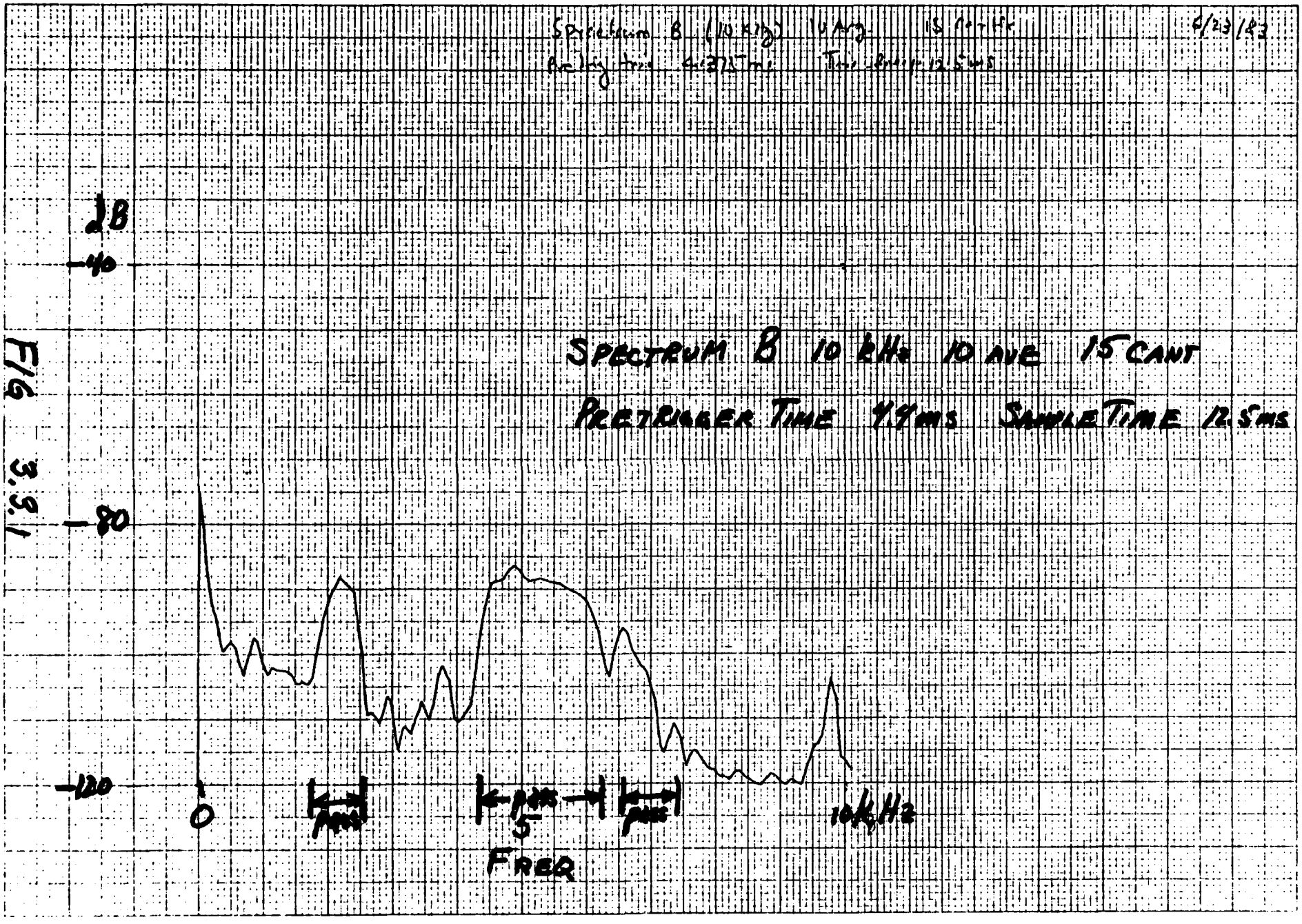

Fig 3.9.1

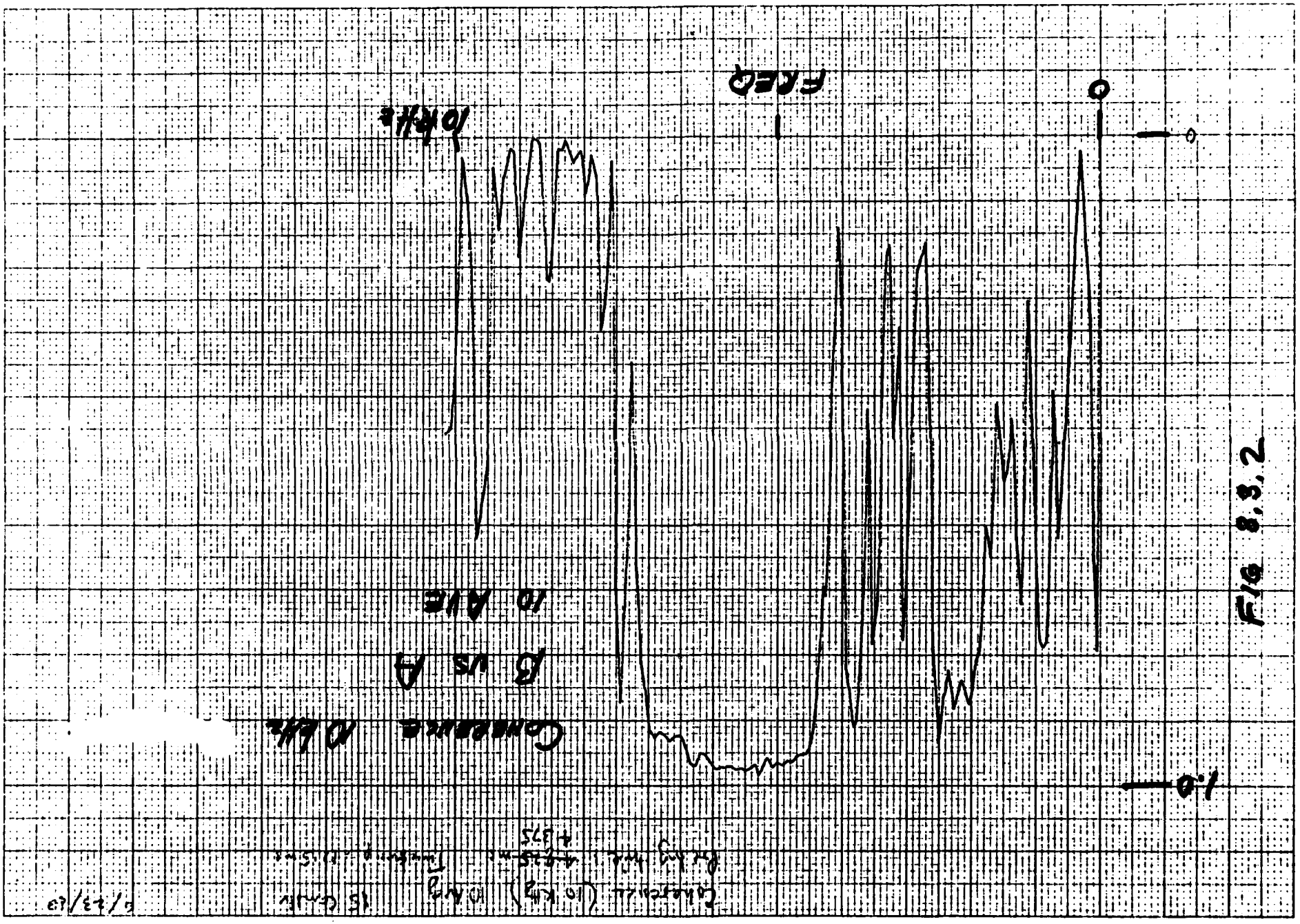

Fig 8.3.2

Spectrum B 5 KHz 10 Avg 15 Cents 6/24/83

Prefrig time 6.5 ms Time per sample 25 ms

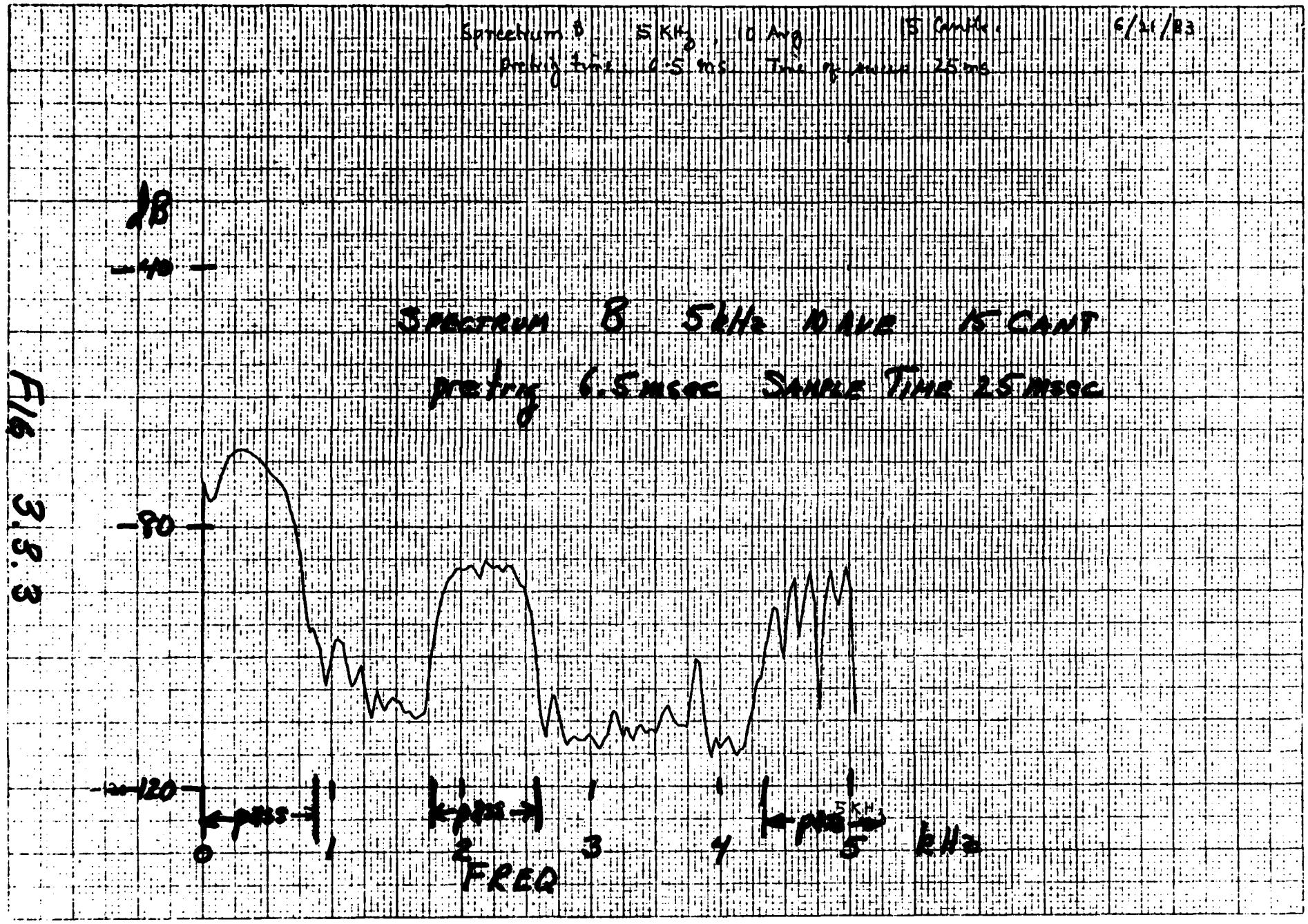

Spectrum B 5KHz 10 AVG 15 CENT

prefrig 6.5 msec Sample Time 2.5 msec

Fig 3.8.3

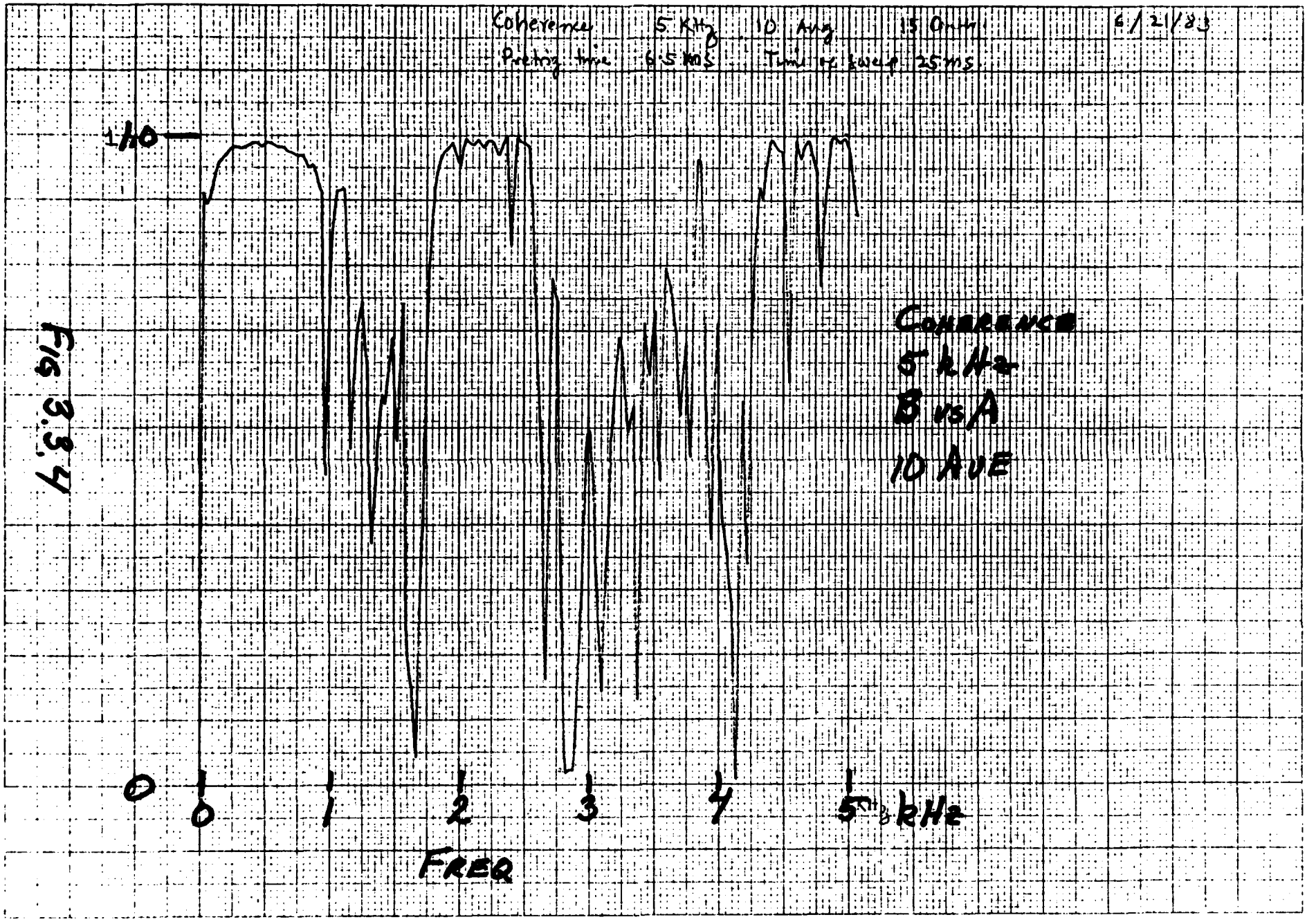

Fig 3.3.4

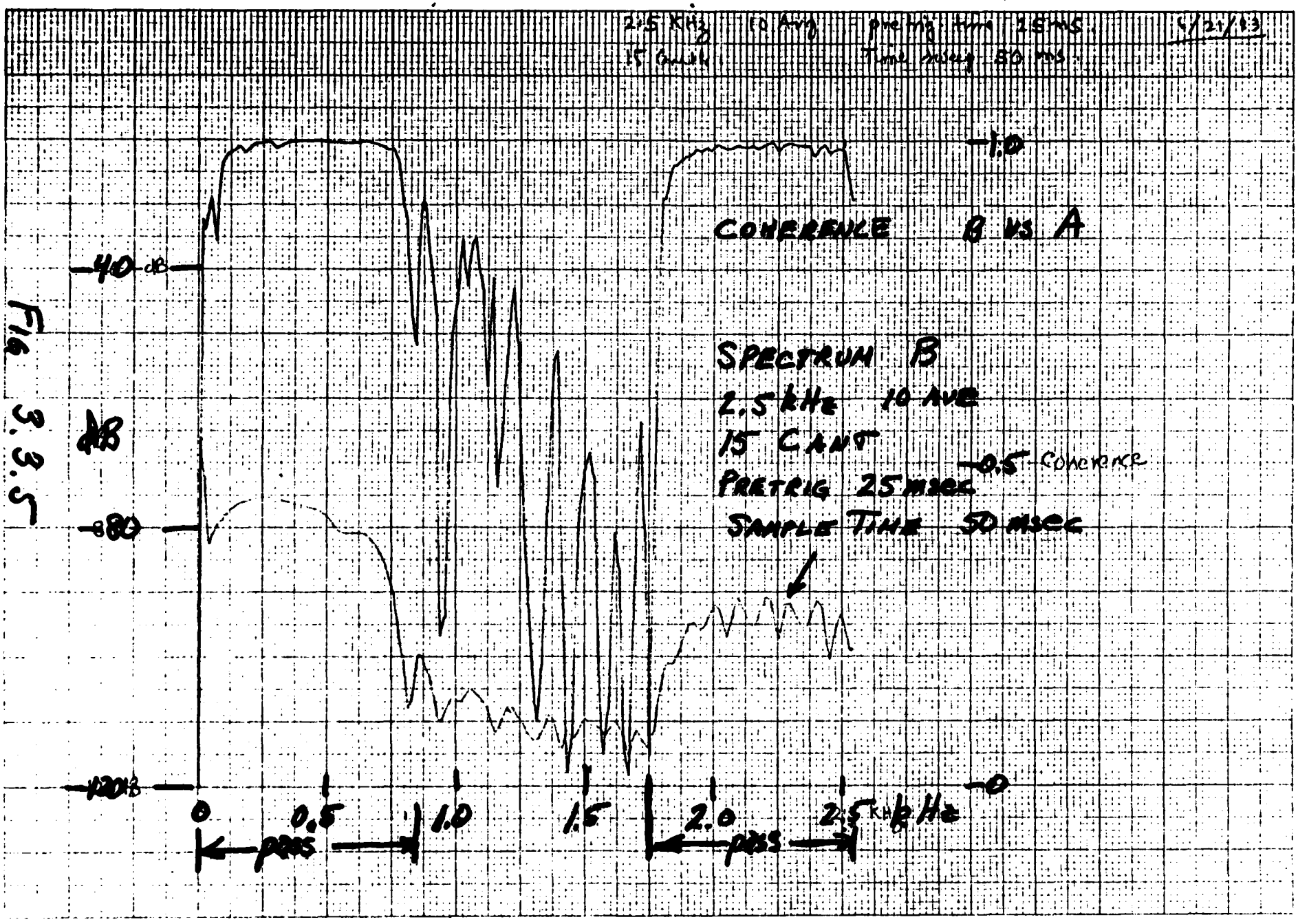

Fig 3.3.5

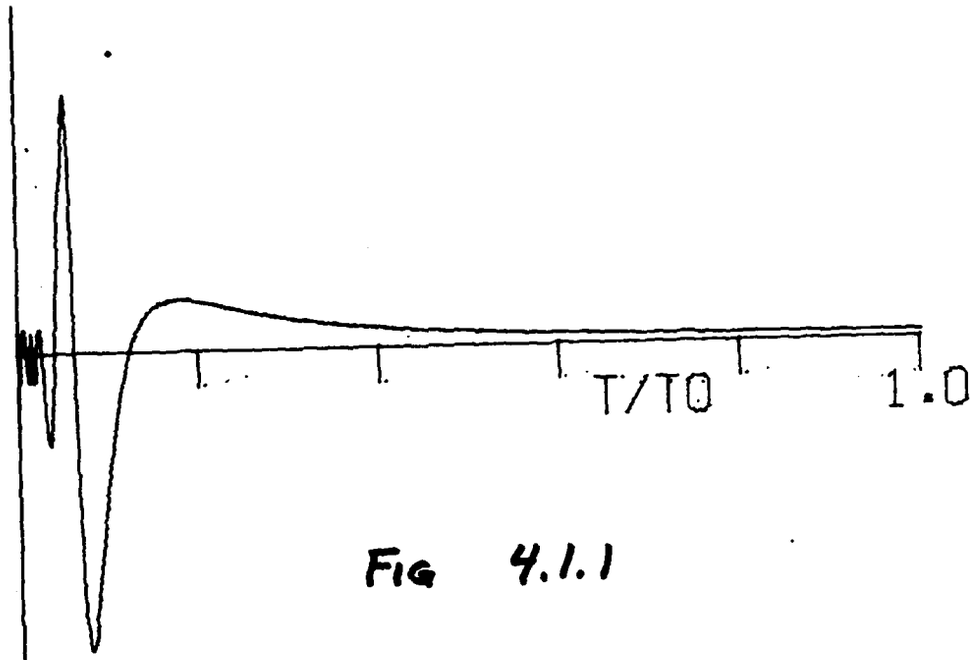

Fig 4.1.1

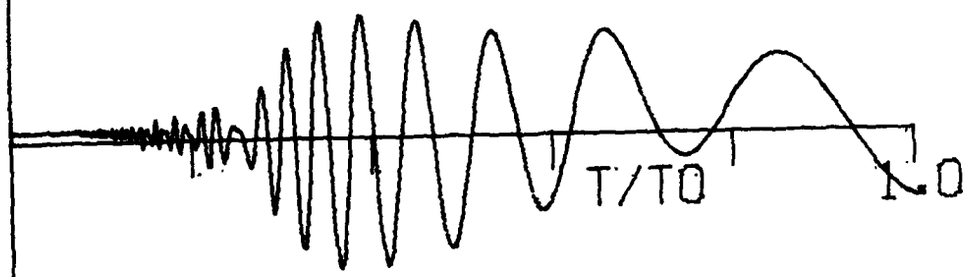

Fig 4.1.2

FIG 2.1.1

END

FILMED

11-83

DTIC